

## A simple Kelvin and Boltzmann viscoelastic analysis of three-dimensional solids by the boundary element method

A.D. Mesquita, H.B. Coda\*

*Structural Engineering Department, São Carlos School of Engineering, University of São Paulo, São Carlos, São Paulo 13566-960, Brazil*

Received 7 September 2002; revised 11 March 2003; accepted 14 March 2003

---

### Abstract

This paper presents a three-dimensional Boundary Element formulation for the analysis of simplified viscoelastic bodies without using internal cells. Two different constitutive models are considered. The first and simplest one is the Kelvin model, which does not consider instantaneous responses. The second, Boltzmann model, considers both instantaneous and viscous behaviour of materials. An appropriate kinematical relation together with differential viscoelastic constitutive representations are employed in order to built the proposed Scheme. Spatial approximations are applied for boundary elements before time solution. The proposed technique results in a time marching process that does not use relaxation (or creep) functions to recover viscous behaviour. Some examples are shown in order to demonstrate the accuracy and stability of the technique when compared to analytical solutions.

© 2003 Elsevier Ltd. All rights reserved.

**Keywords:** Viscoelasticity; Boundary elements; Numerical time integration

---

### 1. Introduction

Alternative general viscoelastic procedures to solve two-dimensional (2D) problems had been developed by the authors in recent works [1–4]. These formulations are based on differential viscoelastic constitutive relations. When general viscoelasticity had been considered it was required to employ internal cells in order to take into account viscous behaviours of materials by the BEM formulation [1,2]. Recently, introducing a further simplification into the viscous constitutive relations [2,8] it has been possible, after a big algebraic effort, extent this kind of formulation to deal with 2D viscous problems without internal cells [3,4]. Encouraged by the absence of cells the authors extended here the previous procedure considering three-dimensional (3D) applications. For exterior problems, even for 2D applications, the advantages of the BEM formulation over its counterpart FEM are clearly evident [4,5]. These advantages justify the effort employed in developing the 3D viscoelastic formulation presented as a first time in this work.

It is important to note that the proposed technique is different from classical viscoelastic ones and is an

interesting alternative for them due to the simplicity of the resulting time marching process. The usual numerical viscoelastic analysis are based on relaxation functions [6–9] together with a convenient incremental scheme where the convolutional aspect of the viscous behaviour is transformed into discrete contributions to the elastic response. These incremental techniques calculate viscous residuals (point by point) by stress decay considerations (like viscoplastic processes [10–12]) while the proposed scheme solves the viscous behaviour in a differential system of equations where displacement and velocities are directly related. One cannot forget valuable contributions in literature related to viscoelastic quasi-static and dynamic problems [17–35], most of these references are worried with complete viscosity representation.

An important characteristic of the proposed technique is that the experimental results for creep and relaxation functions [5] can be employed to achieve the necessary viscous parameters used into differential constitutive relations.

Section 4 shows various examples in order to demonstrate the accuracy and stability of the formulation. Analytical solutions are taken for comparison because they are the natural accuracy reference parameter. It is not possible, from the consulted literature, to compare

\* Corresponding author. Tel./fax: +55-16-2739482.

E-mail addresses: [hbcoda@sc.usp.br](mailto:hbcoda@sc.usp.br) (H.B. Coda); [mesquita@sc.usp.br](mailto:mesquita@sc.usp.br) (A.D. Mesquita).

the performance of this technique with others, because no data about time processing or stability are given in references. Along all text Einstein notation is adopted.

## 2. Basic relations for viscoelasticity

This section is divided into two main parts, one related to the Kelvin model and other related to the Boltzmann standard relations.

### 2.1. Kelvin model

Using rheological models defined in the uniaxial space is the usual way adopted to describe the viscoelastic behaviour of solids. The Kelvin–Voigt viscoelastic representation is very often used to describe this kind of behaviour, see Fig. 1. The understanding of this simple model is a basic step to develop more complicated ones, as for example the Boltzmann model described in the next item.

From Fig. 1, the following relations are stated

$$\varepsilon_{ij} = \varepsilon_{ij}^e = \varepsilon_{ij}^v \quad (1)$$

$$\sigma_{ij} = \sigma_{ij}^e + \sigma_{ij}^v \quad (2)$$

where  $\varepsilon$  and  $\sigma$  are the strain and stress tensors; the Cartesian co-ordinates are represented by subscripts  $i$  and  $j$ , while the superscript  $v$  and  $e$  represent viscous and elastic parts, respectively.

The elastic stress can be written in terms of strain components, as follows

$$\sigma_{ij}^e = C_{ij}^{lm} \varepsilon_{lm}^e = C_{ij}^{lm} \varepsilon_{lm} \quad (3)$$

Similarly, the following relation gives the viscous stress components:

$$\sigma_{ij}^v = \eta_{ij}^{lm} \dot{\varepsilon}_{lm}^v = \eta_{ij}^{lm} \dot{\varepsilon}_{lm} \quad (4)$$

In Eqs. (3) and (4),  $C_{ij}^{lm}$  and  $\eta_{ij}^{lm}$  contain the elastic compliance factors and the viscous constitutive parameters, respectively, defined as follows

$$C_{ij}^{lm} = \lambda \delta_{ij} \delta_{lm} + \mu (\delta_{il} \delta_{jm} + \delta_{im} \delta_{jl}) \quad (5)$$

$$\eta_{ij}^{lm} = \theta_\lambda \lambda \delta_{ij} \delta_{lm} + \theta_\mu \mu (\delta_{il} \delta_{jm} + \delta_{im} \delta_{jl}) \quad (6)$$

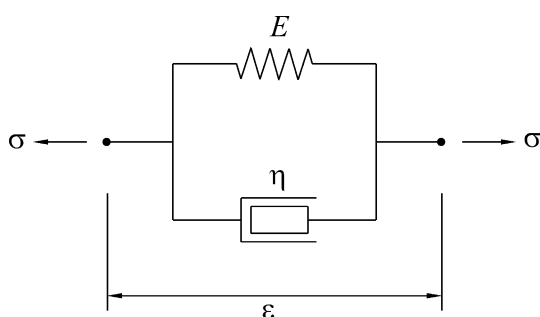


Fig. 1. Kelvin–Voigt viscoelastic model (uniaxial representation).

where  $\lambda$  and  $\mu$  are the Lamé's constants, given by

$$\lambda = \frac{\nu E}{(1 + \nu)(1 - 2\nu)} \quad (7)$$

$$\mu = G = \frac{E}{2(1 + \nu)} \quad (8)$$

in which  $E$  and  $\nu$  are the Young modulus and Poisson ratio, respectively, while  $\theta_\lambda$  and  $\theta_\mu$  are the hydrostatic and deviatoric viscosity coefficients.

Replacing Eqs. (3) and (4) into Eq. (2) gives:

$$\sigma_{ij} = C_{ij}^{lm} \varepsilon_{lm} + \eta_{ij}^{lm} \dot{\varepsilon}_{lm} \quad (9a)$$

In this work, a further simplification is assumed, i.e.  $\theta_\lambda = \theta_\mu = \gamma$ , in order to obtain only boundary values at the integral equations, see Section 3.

$$\sigma_{ij} = C_{ij}^{lm} \varepsilon_{lm} + \gamma C_{ij}^{lm} \dot{\varepsilon}_{lm} \quad (9b)$$

This simplification can be acceptable for some application as, for example, internal pressure inside cavities, see numerical proof in Ref. [1], where the particular stress state determines that  $\theta_\mu$  has a predominant influence. The simplification can also be adopted for certain materials were the proximity of viscous parameters is really true. For general problems one can use internal cells [1] in the region were both parameters are important and only one parameter, preferentially  $\theta_\mu$ , for the remaining part of the body. Viscous effects will be incorporated into the equilibrium equation of the body by numerically relating strain time rates with material velocity in a way that the viscous characteristics of the body satisfy boundary conditions together with the elastic ones.

In order to do this, one can write the actual equilibrium equation for an infinitesimal part of a general viscoelastic body, as follows

$$\sigma_{ij,i} + b_j = \rho \ddot{u}_j + c \dot{u}_j \quad (10)$$

or

$$\sigma_{ij,i}^e + \sigma_{ij,i}^v + b_j = \rho \ddot{u}_j + c \dot{u}_j \quad (11)$$

where  $b_j$  is the body force acting in  $j$  direction.

Note that Eq. (11) exhibits explicitly the viscous stress term which plays an important role in the body equilibrium. As in this work the dynamic effects, inertia forces and friction, will not be considered, expression (11) should be rewritten as:

$$\sigma_{ij,i}^e + \sigma_{ij,i}^v + b_j = 0 \quad (12)$$

### 2.2. Boltzmann model

Another representation employed to describe the mechanical behaviour of viscoelastic materials, stress/strain constitutive relation, is the so-called standard Boltzmann

model. This model is more general than the previous one, and can be described in a uniaxial representation as shown in Fig. 2.

This model is represented by a serial arrangement of a Kelvin–Voigt model and an elastic relation. It can reproduce both the instantaneous and the viscous behaviour of a specific material.

It is easy to observe, see Fig. 2, that the stress level for each part of the model, elastic and viscoelastic, is the same  $\sigma_{ij} = \sigma_{ij}^e = \sigma_{ij}^{ve}$  (13)

where  $\sigma_{ij}$ ,  $\sigma_{ij}^e$  and  $\sigma_{ij}^{ve}$  are, respectively, total, elastic and viscoelastic stress parts. The total strain can be decomposed into its elastic and viscoelastic parts, i.e.:

$$\varepsilon_{lm} = \varepsilon_{lm}^e + \varepsilon_{lm}^{ve} \quad (14)$$

From Fig. 2, one may observe that the viscoelastic stress is the summation of a viscous and an elastic part, as follows

$$\sigma_{ij}^{ve} = \sigma_{ij}^{el} + \sigma_{ij}^v \quad (15)$$

where  $\sigma_{ij}^v$  is the viscous part and  $\sigma_{ij}^{el}$  is the elastic part of the stress developed in the Kelvin–Voigt fragment of the Boltzmann model.

From previous equations, one is able to define the differential constitutive relation necessary to build the desired boundary integral equations [4]

$$\begin{aligned} \sigma_{qs} = & \left( \frac{E_{ve} E_e}{E_{ve} + E_e} \right) \tilde{C}_{qs}^{\gamma k} \varepsilon_{\gamma k} + \left( \frac{E_e E_{ve}}{E_{ve} + E_e} \right) \tilde{\eta}_{qs}^{\gamma k} \dot{\varepsilon}_{\gamma k} \\ & - \left( \frac{E_{ve}}{E_{ve} E_e} \right) \tilde{\eta}_{qs}^{ij} \tilde{D}_{ij}^{\gamma k} \dot{\sigma}_{\gamma k} \end{aligned} \quad (16)$$

where  $\tilde{C}_{ij}^{lm}$ ,  $\tilde{\eta}_{qs}^{\gamma k}$ , and  $\tilde{D}_{ij}^{\gamma k}$  are, respectively, the dimensionless constitutive tensor, the dimensionless viscoelastic compliance tensor and the inverse of the dimensionless constitutive tensor [4].

As described for the Kelvin model, in order to write an integral statement with only boundary values it is necessary to impose the simplification  $\theta_\lambda = \theta_\mu = \gamma$ . In this way expression (16) turns into:

$$\begin{aligned} \sigma_{ij} = & \left( \frac{E_{ve} E_e}{E_{ve} + E_e} \right) \tilde{C}_{ij}^{lm} \varepsilon_{lm} + \left( \frac{\gamma E_{ve} E_e}{E_{ve} + E_e} \right) \tilde{C}_{ij}^{lm} \dot{\varepsilon}_{lm} \\ & - \left( \frac{\gamma E_{ve}}{E_{ve} E_e} \right) \dot{\sigma}_{ij} \end{aligned} \quad (17)$$

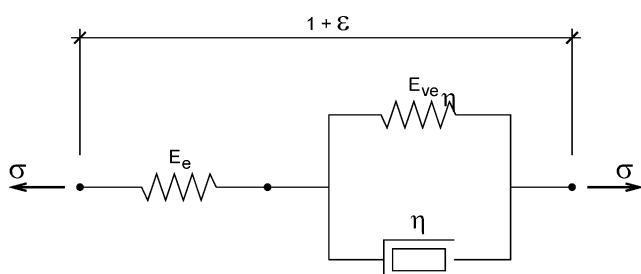


Fig. 2. Boltzmann viscoelastic model (uniaxial representation).

This is the general rheological differential relation for the Boltzmann model. More complicate rheological models can be introduced following similar procedures, each new dashpots/spring chain will deserve a new research, i.e. a big algebraic effort to build the proper relations. And it is more difficult to do without using cells (simplified constitutive relation) than using cells or using finite elements (complete model). The viscous parameter  $\gamma$  can vary along time and are calculated from creep and relaxation functions. Therefore, the developed formulation is valid even for ageing viscosity [5,6,8].

### 3. Integral equations

The boundary element method is based on boundary integral equations. In order to be clear, this section is separated into two main subsections. The first subsection develops the integral statement for Kelvin model, due to its simplicity. In the second subsection, the proposed procedure is extended to the Boltzmann model.

#### 3.1. Kelvin model

##### 3.1.1. Displacement representation

The viscoelastic integral equation for boundary or internal points is obtained here using the weighting residual technique on the differential equilibrium equation (12) written in the following form:

$$\sigma_{ij,j} + b_i = 0 \quad (18)$$

The error present in Eq. (18), when an approximate solution is adopted, can be weighted by a proper function. In this work, the Kelvin fundamental solution for elastic infinite body is adopted [13]. Eq. (18) is weighted over the analysed domain  $\Omega$ , as follows

$$\int_{\Omega} u_{ki}^* (\sigma_{ij,j} + b_i) d\Omega = 0 \quad (19)$$

where  $u_{ki}^*$  is the Kelvin fundamental solution. It represents the effect of a unit concentrate load applied at a point located in an infinite domain. Applying the divergence theorem on the first term of Eq. (19), one achieves

$$\int_{\Gamma} u_{ki}^* \sigma_{ij,j} n_j d\Gamma - \int_{\Omega} u_{ki,j}^* \sigma_{ij} d\Omega + \int_{\Omega} u_{ki}^* b_i d\Omega = 0 \quad (20)$$

where  $\Gamma$  is the boundary of the analysed body and  $n_j$  is the outward normal vector component. Knowing that,  $\sigma_{ij,j} n_j = p_i$  and that  $u_{ki,j}^* \sigma_{ij} = \varepsilon_{kij}^* \sigma_{ij}$ , where  $\varepsilon_{kij}^*$  is the strain fundamental term, Eq. (20) turns into:

$$\int_{\Gamma} u_{ki}^* p_i d\Gamma - \int_{\Omega} \varepsilon_{kij}^* \sigma_{ij} d\Omega + \int_{\Omega} u_{ki}^* b_i d\Omega = 0 \quad (21)$$

This equation is the starting point to obtain viscoelastic integral representations. Imposing viscoelastic relations,

Eq. (9b), on Eq. (21), results:

$$\int_{\Gamma} u_{ki}^* p_i d\Gamma - \int_{\Omega} \varepsilon_{kij}^* C_{ij}^{lm} \varepsilon_{lm} d\Omega - \int_{\Omega} \varepsilon_{kij}^* \gamma C_{ij}^{lm} \dot{\varepsilon}_{lm} d\Omega + \int_{\Omega} u_{ki}^* b_i d\Omega = 0 \quad (22)$$

Knowing that

$$\varepsilon_{kij}^* C_{ij}^{lm} \varepsilon_{lm} = \sigma_{klm}^* \varepsilon_{lm} = \sigma_{klm}^* u_{l,m} = \sigma_{kij}^* u_{i,j} \quad (23)$$

$$\varepsilon_{kij}^* \gamma C_{ij}^{lm} \dot{\varepsilon}_{lm} = \gamma \sigma_{klm}^* \dot{\varepsilon}_{lm} = \gamma \sigma_{klm}^* \dot{u}_{l,m} = \gamma \sigma_{kij}^* \dot{u}_{i,j} \quad (24)$$

Eq. (22) turns into:

$$\int_{\Gamma} u_{ki}^* p_i d\Gamma - \int_{\Omega} \sigma_{kij}^* u_{i,j} d\Omega - \gamma \int_{\Omega} \sigma_{kij}^* \dot{u}_{i,j} d\Omega + \int_{\Omega} u_{ki}^* b_i d\Omega = 0 \quad (25)$$

Integrating by parts, the second and third terms of Eq. (25) one achieves:

$$\int_{\Gamma} u_{ki}^* p_i d\Gamma - \int_{\Gamma} \sigma_{kij}^* n_j u_i d\Gamma + \int_{\Omega} \sigma_{kij,j}^* u_i d\Omega - \gamma \int_{\Gamma} \sigma_{kij}^* n_j \dot{u}_i d\Gamma + \gamma \int_{\Omega} \sigma_{kij,j}^* \dot{u}_i d\Omega + \int_{\Omega} u_{ki}^* b_i d\Omega = 0 \quad (26)$$

Eq. (26) can be rewritten by using the fundamental equilibrium equation, i.e.

$$\sigma_{kij,j}^* = -\delta(p, s) \delta_{ki} \quad (27)$$

where  $\delta(p, s)$  is the Dirac's Delta distribution,  $s$  is a field point and  $p$  is the source location. Applying Eq. (27) into Eq. (26), taking into consideration the Dirac's Delta properties and that  $\sigma_{kij,j}^* = p_{ki}^*$ , results:

$$\bar{C}_{ki} u_i(p) + \gamma \bar{C}_{ki} \dot{u}_i(p) = \int_{\Gamma} u_{ki}^* p_i d\Gamma - \int_{\Gamma} p_{ki}^* u_i d\Gamma - \gamma \int_{\Gamma} p_{ki}^* \dot{u}_i d\Gamma + \int_{\Omega} u_{ki}^* b_i d\Omega \quad (28)$$

The term  $\bar{C}_{ki}$  is the same obtained in the elastostatic formulations and can be found in standard boundary element Refs. [13,14]. Eq. (28) is the alternative viscoelastic integral representation for the Kelvin–Voigt model. The body force domain integral can be easily transformed into its boundary representation, resulting an expression written exclusively for boundary values [15]. If the body force  $b_i$  is constant, the explicit integral expression is written as:

$$\begin{aligned} \int_{\Omega} u_{ki}^* b_i d\Omega &= b_i \int_{\Omega} u_{ki}^* d\Omega = b_i \int_{\theta} \int_r u_{ki}^* r dr d\theta \\ &= b_i \int_{\Gamma} \int_r u_{ki}^* r dr \frac{1}{r} \frac{\partial r}{\partial n} d\Gamma = b_i \int_{\Gamma} B_{ki}^* d\Gamma \end{aligned} \quad (29)$$

For Kelvin fundamental solution,  $B_{ki}^*$  is given by:

$$B_{ki}^* = \frac{r}{16\pi G(1-\nu)} \times \left[ (4\nu-3) \left( \ln r - \frac{1}{2} \right) \delta_{ki} + r_{,k} r_{,i} \right] \frac{\partial r}{\partial n} \quad (30)$$

Rewriting Eq. (28) results:

$$\bar{C}_{ki} u_i(p) + \gamma \bar{C}_{ki} \dot{u}_i(p) = \int_{\Gamma} u_{ki}^* p_i d\Gamma - \int_{\Gamma} p_{ki}^* u_i d\Gamma - \gamma \int_{\Gamma} p_{ki}^* \dot{u}_i d\Gamma + b_i \int_{\Gamma} B_{ki}^* d\Gamma \quad (31)$$

It is worth to note that necessary kernels are given in Appendix A.

### 3.1.2. Stress integral representation for internal points

To write the stress integral representation for internal points one starts by achieving the strain integral representation. At internal points the displacement integral representation is given by:

$$u_k(p) + \gamma \dot{u}_k(p) = \int_{\Gamma} u_{ki}^* p_i d\Gamma - \int_{\Gamma} p_{ki}^* u_i d\Gamma - \gamma \int_{\Gamma} p_{ki}^* \dot{u}_i d\Gamma + b_i \int_{\Gamma} B_{ki}^* d\Gamma \quad (32)$$

The kinematical relations for small strain and strain time rate (strain velocity), are adopted:

$$\varepsilon_{ke} = \frac{1}{2}(u_{k,e} + u_{e,k}) \quad (33a)$$

$$\dot{\varepsilon}_{ke} = \frac{1}{2}(\dot{u}_{k,e} + \dot{u}_{e,k}) \quad (33b)$$

The last relation is not usual in literature of solid analysis and posses a key importance in the proposed scheme. Applying the above definitions on Eq. (32) and considering that the derivatives are done with respect to the source point location, one finds:

$$\varepsilon_{ke}(p) + \gamma \dot{\varepsilon}_{ke}(p) = \int_{\Gamma} \varepsilon_{kie}^* p_i d\Gamma - \int_{\Gamma} \hat{p}_{kie}^* u_i d\Gamma - \gamma \int_{\Gamma} \hat{p}_{kie}^* \dot{u}_i d\Gamma + b_i \int_{\Gamma} \hat{B}_{kie}^* d\Gamma \quad (34)$$

The total stress is obtained using the constitutive relation (9b) over Eq. (34), resulting:

$$\sigma_{pq}^e(p) + \sigma_{pq}^v(p) = \int_{\Gamma} \bar{\sigma}_{piq}^* p_i d\Gamma - \int_{\Gamma} \bar{p}_{piq}^* u_i d\Gamma - \gamma \int_{\Gamma} \bar{p}_{piq}^* \dot{u}_i d\Gamma + b_i \int_{\Gamma} \bar{B}_{piq}^* d\Gamma \quad (35)$$

Using Eq. (2), Eq. (35) turns into

$$\begin{aligned} \sigma_{pq}(p) &= \int_{\Gamma} \bar{\sigma}_{piq}^* p_i d\Gamma - \int_{\Gamma} \bar{p}_{piq}^* u_i d\Gamma - \gamma \int_{\Gamma} \bar{p}_{piq}^* \dot{u}_i d\Gamma \\ &\quad + b_i \int_{\Gamma} \bar{B}_{piq}^* d\Gamma \end{aligned} \quad (36)$$

where  $\bar{\sigma}_{piq}^*$ ,  $\bar{p}_{piq}^*$ , and  $\bar{B}_{piq}^*$  are defined in Appendix A.

In order to determine the elastic and viscous stresses, from Eq. (36), one should apply a special scheme for which Eq. (3) is written in the following form:

$$\dot{\sigma}_{ij}^e = C_{ij}^{lm} \dot{\varepsilon}_{lm}^e = \frac{1}{\gamma} \gamma C_{ij}^{lm} \dot{\varepsilon}_{lm}^e = \frac{1}{\gamma} \sigma_{ij}^v \Rightarrow \sigma_{ij}^v = \gamma \dot{\sigma}_{ij}^e \quad (37)$$

Substituting the above relation into Eq. (2) one achieves the following time differential equation:

$$\gamma \dot{\sigma}_{ij}^e + \sigma_{ij}^e - \sigma_{ij} = 0 \quad (38)$$

In this work, Eq. (38) is solved numerically by adopting linear approximation for elastic stress. This numerical procedure is shown in the next item.

### 3.1.3. Algebraic treatment

The kernels present in Eqs. (32) and (36) are the usual ones of ordinary static boundary element formulations. The boundary  $\Gamma$  of the analysed domain is divided into various boundary elements  $\Gamma_c$ , over which the variables are approximated, as follows

$$\begin{aligned} p_i &= \phi^\alpha P_i^\alpha \\ u_i &= \phi^\alpha U_i^\alpha \\ \dot{u}_i &= \phi^\alpha \dot{U}_i^\alpha \end{aligned} \quad (39)$$

where  $\phi^\alpha$  are shape functions and  $\alpha$  are element nodes. The values  $P_i^\alpha$ ,  $U_i^\alpha$  and  $\dot{U}_i^\alpha$  are nodal variables. Adopting these approximations the integral representation for displacement and stress are written as:

$$\begin{aligned} \bar{C}_{ki} U_i(p) + \gamma \bar{C}_{ki} \dot{U}_i(p) \\ = \sum_{c=1}^{n_c} \int_{\Gamma_c} u_{ki}^* \phi^\alpha d\Gamma_c P_i^\alpha - \sum_{c=1}^{n_c} \int_{\Gamma_c} p_{ki}^* \phi^\alpha d\Gamma_c U_i^\alpha \\ - \gamma \sum_{c=1}^{n_c} \int_{\Gamma_c} p_{ki}^* \phi^\alpha d\Gamma_c \dot{U}_i^\alpha + b_i \sum_{c=1}^{n_c} \int_{\Gamma_c} B_{ki}^* d\Gamma_c \quad (40) \end{aligned}$$

$$\begin{aligned} \sigma_{pq}(p) &= \sum_{c=1}^{n_c} \int_{\Gamma_c} \bar{\sigma}_{piq}^* \phi^\alpha d\Gamma_c P_i^\alpha \\ &- \sum_{c=1}^{n_c} \int_{\Gamma_c} \bar{p}_{piq}^* \phi^\alpha d\Gamma_c U_i^\alpha \\ &- \gamma \sum_{c=1}^{n_c} \int_{\Gamma_c} \bar{p}_{piq}^* \phi^\alpha d\Gamma_c \dot{U}_i^\alpha \\ &+ b_i \sum_{c=1}^{n_c} \int_{\Gamma_c} \bar{B}_{piq}^* d\Gamma_c \quad (41) \end{aligned}$$

After chosen the number of source points equal to the number of nodes and calculating all integrals, results

$$H U(t) + \gamma H \dot{U}(t) = G P(t) + B b(t) \quad (42)$$

$$\sigma(t) = G' P(t) - H' U(t) - \gamma H' \dot{U}(t) + B' b(t) \quad (43)$$

where  $t$  represents time.

To solve the time differential matrix Eq. (42) it is necessary to approximate velocity along time. This is done adopting linear time approximation, as follows:

$$\dot{U}_{s+1} = \frac{U_{s+1} - U_s}{\Delta t} \quad (44)$$

Applying Eq. (44) into Eq. (42) the following linear time marching process is achieved

$$\bar{H} U_{s+1} = G P_{s+1} + F_s \quad (45)$$

where

$$\bar{H} = \left( 1 + \frac{\gamma}{\Delta t} \right) H \quad (46)$$

$$F_s = \frac{\gamma}{\Delta t} H U_s + B b_{s+1} \quad (47)$$

As past values are known, it is necessary only to solve the system (45) for actual time, i.e.  $t_{s+1}$ , and go to the next time step. The boundary conditions along time are prescribed by interchanging columns of  $\bar{H}$  and  $G$ .

In order to calculate the total stress one applies Eq. (44) into Eq. (43), written for the instant  $t_{s+1}$ , as follows:

$$\sigma_{s+1} = G' P_{s+1} - H' U_{s+1} - \gamma H' \dot{U}_{s+1} + B' b_{s+1} \quad (48)$$

Assuming the same approximation for elastic stress as the one adopted for velocity, i.e.:

$$\dot{\sigma}_{s+1}^e = \frac{\sigma_{s+1}^e - \sigma_s^e}{\Delta t} \quad (49)$$

and substituting Eq. (49) into Eq. (38) results:

$$\sigma_{s+1}^e = \left( \sigma_{s+1} + \frac{\gamma}{\Delta t} \sigma_s^e \right) / \left( 1 + \frac{\gamma}{\Delta t} \right) \quad (50)$$

As  $\sigma_s^e$  is known and  $\sigma_{s+1}$  is obtained by Eq. (48), the elastic stress holds from Eq. (50) and the viscous part comes from Eq. (2), completing the procedure.

### 3.2. Boltzmann model

In this section, the viscoelastic formulation previously developed for the Kelvin model is extended to include the Boltzmann viscoelastic relation.

Applying the weighting residual technique over the differential equilibrium equation (18) the following integral equation is achieved

$$\int_{\Gamma} u_{ki}^* p_i d\Gamma - \int_{\Omega} \varepsilon_{ij}^* \sigma_{ij} d\Omega + \int_{\Omega} u_{ki}^* b_i d\Omega = 0 \quad (51)$$

This is the same equation used in Section 3.1. Imposing on Eq. (51) the rheological relation (17) one

achieves:

$$\begin{aligned} \int_{\Gamma} u_{ki}^* p_i d\Gamma - \frac{E_e E_{ve}}{E_e + E_{ve}} \int_{\Omega} \varepsilon_{kij}^* C_{ij}^{lm} \varepsilon_{lm} d\Omega \\ - \frac{\gamma E_e E_{ve}}{E_e + E_{ve}} \int_{\Omega} \varepsilon_{kij}^* C_{ij}^{lm} \dot{\varepsilon}_{lm} d\Omega \\ + \frac{\gamma E_{ve}}{E_e + E_{ve}} \int_{\Omega} \varepsilon_{kij}^* \dot{\sigma}_{ij} d\Omega + \int_{\Omega} u_{ki}^* b_i d\Omega = 0 \end{aligned} \quad (52)$$

Following the steps described for 2D formulation [4] one achieves the displacement integral equation for Boltzmann model, as:

$$\begin{aligned} \bar{C}_{ki} u_i(p) + \gamma \bar{C}_{ki} \dot{u}_i(p) = \frac{E_e + E_{ve}}{E_{ve}} \int_{\Gamma} u_{ki}^* p_i d\Gamma \\ - \int_{\Gamma} p_{ki}^* u_i d\Gamma - \gamma \int_{\Gamma} p_{ki}^* \dot{u}_i d\Gamma \\ + \gamma \left[ \int_{\Gamma} u_{ki}^* \dot{p}_i d\Gamma + b_i \int_{\Gamma} B_{ki}^* d\Gamma \right] \\ + \frac{E_e + E_{ve}}{E_{ve}} b_i \int_{\Gamma} B_{ki}^* d\Gamma \end{aligned} \quad (53)$$

The stress integral representation for total stress following the Boltzmann viscoelastic model is achieved following the same steps described for the Kelvin model, keeping in mind Eq. (17), as follows:

$$\begin{aligned} \sigma_{pq}(p) = \int_{\Gamma} \bar{\sigma}_{piq}^* p_i d\Gamma - \frac{E_{ve}}{E_e + E_{ve}} \int_{\Gamma} \bar{p}_{piq}^* u_i d\Gamma \\ - \frac{\gamma E_{ve}}{E_e + E_{ve}} \int_{\Gamma} \bar{p}_{piq}^* \dot{u}_i d\Gamma \\ + \frac{\gamma E_{ve}}{E_e + E_{ve}} \left[ \int_{\Gamma} \bar{\sigma}_{piq}^* \dot{p}_i d\Gamma + b_i \int_{\Gamma} \bar{B}_{piq}^* d\Gamma \right] \\ + b_i \int_{\Gamma} \bar{B}_{piq}^* d\Gamma - \frac{\gamma E_{ve}}{E_e + E_{ve}} \dot{\sigma}_{pq}(p) \end{aligned} \quad (54)$$

The functions  $\bar{p}_{piq}^*$ ,  $\bar{\sigma}_{piq}^*$  and  $\bar{B}_{piq}^*$  were defined previously for the Kelvin model. The elastic instantaneous stress and the viscoelastic stress are equal to the total stress, given by Eq. (54), see Eqs. (13) and (15). It is necessary to separate the viscous and elastic parts of the viscoelastic stress. This is done using the following relation [3,4]:

$$\dot{\sigma}_{ij}^{\text{el}} = C_{ij}^{lm} \dot{\varepsilon}_{lm}^{\text{ve}} = \frac{1}{\gamma} \gamma C_{ij}^{lm} \dot{\varepsilon}_{lm}^{\text{ve}} = \frac{1}{\gamma} \sigma_{ij}^{\text{v}} \Rightarrow \sigma_{ij}^{\text{v}} = \gamma \dot{\sigma}_{ij}^{\text{el}} \quad (55)$$

Substituting Eq. (55) into Eq. (15) results the following differential equation

$$\gamma \dot{\sigma}_{ij}^{\text{el}} + \sigma_{ij}^{\text{el}} - \sigma_{ij} = 0 \quad (56)$$

This equation is similar to Eq. (38) written for the Kelvin model, but now it is understood in the Boltzmann model sense. This equation is solved numerically by adopting a proper time approximation for the elastic stress rate.

### 3.2.1. Algebraic treatment

The kernels to be integrated in Eqs. (53) and (54) are the same usually found in elastic boundary elements formulations. Adopting the same approximations used for

the Kelvin model and including the following approximation for surface force rate

$$\dot{p}_i = \phi^\alpha \dot{P}_i^\alpha \quad (57)$$

one writes

$$\begin{aligned} \bar{C}_{ki} U_i(p) = \frac{E_e + E_{ve}}{E_{ve}} \sum_{c=1}^{n_c} \int_{\Gamma_c} u_{ki}^* \phi^\alpha d\Gamma_c P_i^\alpha \\ - \sum_{c=1}^{n_c} \int_{\Gamma_c} p_{ki}^* \phi^\alpha d\Gamma_c U_i^\alpha \\ - \gamma \sum_{c=1}^{n_c} \int_{\Gamma_c} p_{ki}^* \phi^\alpha d\Gamma_c \dot{U}_i^\alpha - \gamma \bar{C}_{ki} \dot{U}_i(p) \\ + \gamma \sum_{c=1}^{n_c} \int_{\Gamma_c} u_{ki}^* \phi^\alpha d\Gamma_c \dot{P}_i^\alpha \\ + \gamma \sum_{c=1}^{n_c} \int_{\Gamma_c} B_{ki}^* d\Gamma_c \dot{b}_i \\ + \frac{E_e + E_{ve}}{E_{ve}} \sum_{c=1}^{n_c} \int_{\Gamma_c} B_{ki}^* d\Gamma_c b_i \end{aligned} \quad (58)$$

$$\begin{aligned} \sigma_{pq}(p) = \sum_{c=1}^{n_c} \int_{\Gamma_c} \bar{\sigma}_{piq}^* \phi^\alpha d\Gamma_c P_i^\alpha \\ - \frac{E_{ve}}{E_e + E_{ve}} \sum_{c=1}^{n_c} \int_{\Gamma_c} \bar{p}_{piq}^* \phi^\alpha d\Gamma_c U_i^\alpha \\ - \frac{\gamma E_{ve}}{E_e + E_{ve}} \sum_{c=1}^{n_c} \int_{\Gamma_c} \bar{p}_{piq}^* \phi^\alpha d\Gamma_c \dot{U}_i^\alpha \\ + \frac{\gamma E_{ve}}{E_e + E_{ve}} \sum_{c=1}^{n_c} \int_{\Gamma_c} \bar{\sigma}_{piq}^* \phi^\alpha d\Gamma_c \dot{P}_i^\alpha \\ + \frac{\gamma E_{ve}}{E_e + E_{ve}} \sum_{c=1}^{n_c} \int_{\Gamma_c} \bar{B}_{piq}^* d\Gamma_c \dot{b}_i \\ + \sum_{c=1}^{n_c} \int_{\Gamma_c} \bar{B}_{piq}^* d\Gamma_c b_i - \frac{\gamma E_{ve}}{E_e + E_{ve}} \dot{\sigma}_{pq}(p) \end{aligned} \quad (59)$$

After adopting the same number of source points as the nodal ones and performing all spatial integration results

$$\begin{aligned} HU(t) = \frac{E_e + E_{ve}}{E_{ve}} GP(t) - \gamma H \dot{U}(t) + \gamma G \dot{P}(t) + \gamma B \dot{b}(t) \\ + \frac{E_e + E_{ve}}{E_{ve}} B b(t) \end{aligned} \quad (60)$$

$$\begin{aligned} \sigma(t) = G' P(t) - \frac{E_{ve}}{E_e + E_{ve}} H' U(t) - \frac{\gamma E_{ve}}{E_e + E_{ve}} H' \dot{U}(t) \\ + \frac{\gamma E_{ve}}{E_e + E_{ve}} G' \dot{P}(t) + \frac{\gamma E_{ve}}{E_e + E_{ve}} B' \dot{b}(t) + B' b(t) \\ - \frac{\gamma E_{ve}}{E_e + E_{ve}} \dot{\sigma}(t) \end{aligned} \quad (61)$$

where  $t$  represents time.

In order to solve the matrix time differential equation (60) the following time approximations are adopted:

$$\begin{aligned}\dot{U}_{s+1} &= \frac{U_{s+1} - U_s}{\Delta t} \\ \dot{P}_{s+1} &= \frac{P_{s+1} - P_s}{\Delta t} \\ \dot{b}_{s+1} &= \frac{b_{s+1} - b_s}{\Delta t} \\ \dot{\sigma}_{s+1} &= \frac{\sigma_{s+1} - \sigma_s}{\Delta t} \\ \dot{\sigma}_{s+1}^{\text{el}} &= \frac{\sigma_{s+1}^{\text{el}} - \sigma_s^{\text{el}}}{\Delta t}\end{aligned}\quad (62)$$

Introducing the first three approximations of Eqs. (62) into Eq. (61), it turns into a time marching process

$$\bar{H}U_{s+1} = \bar{G}P_{s+1} + F_s \quad (63)$$

where

$$\bar{H} = \left(1 + \frac{\gamma}{\Delta t}\right)H \text{ and } \bar{G} = \left(\frac{\gamma}{\Delta t} + \frac{E_e + E_{ve}}{E_{ve}}\right)G \quad (64)$$

$$\begin{aligned}F_s &= \frac{\gamma}{\Delta t}HU_s - \frac{\gamma}{\Delta t}GP_s \\ &+ B\left[\left(\frac{\gamma}{\Delta t} + \frac{E_e + E_{ve}}{E_{ve}}\right)b_{s+1} - \frac{\gamma}{\Delta t}b_s\right]\end{aligned}\quad (65)$$

The time dependent boundary conditions are prescribed by interchanging columns of  $\bar{H}$  and  $\bar{G}$ . The system (63) is solved for the present instant and the results turns into past for the next time step.

Using the results  $U_{s+1}$  and  $P_{s+1}$ , one is able to calculate  $\dot{P}_{s+1}$ ,  $\dot{U}_{s+1}$  and  $\dot{b}_{s+1}$  following expressions (62). From these values, it is easy (from Eq. (61)) to calculate the total stress level at  $t_{s+1}$  as follows:

$$\begin{aligned}\sigma_{s+1} &= \left(G'P_{s+1} - \frac{E_{ve}}{E_e + E_{ve}}H'U_{s+1} - \frac{\gamma E_{ve}}{E_e + E_{ve}}H'\dot{U}_{s+1}\right. \\ &+ \frac{\gamma E_{ve}}{E_e + E_{ve}}G'\dot{P}_{s+1} + \frac{\gamma E_{ve}}{E_e + E_{ve}}B'\dot{b}_{s+1} + B'b_{s+1} \\ &\left.+ \frac{\gamma}{\Delta t} \frac{E_{ve}}{E_e + E_{ve}}\sigma_s\right) / \left(1 + \frac{\gamma}{\Delta t} \frac{E_{ve}}{E_e + E_{ve}}\right)\end{aligned}\quad (66)$$

The elastic stress at the viscoelastic part of the Boltzmann model  $\dot{\sigma}_{s+1}^{\text{el}}$  is achieved by imposing the approximation shown in Eq. (62) on the differential equation (56), as follows:

$$\sigma_{s+1}^{\text{el}} = \left(\sigma_{s+1} + \frac{\gamma}{\Delta t}\sigma_s^{\text{el}}\right) / \left(1 + \frac{\gamma}{\Delta t}\right) \quad (67)$$

From expression (15) and the elastic part of the viscoelastic stress, Eq. (67), one achieves the viscous stress  $\sigma_{ijv}$ , completing the procedure.

## 4. Examples

In this section four examples related to both Kelvin and Boltzmann models are shown in order to demonstrate the accuracy, stability and generality of the technique when compared to analytical solutions.

### 4.1. Spherical cavity (Kelvin model)

This example consists in a spherical cavity buried in a viscoelastic infinite medium subjected to a suddenly and maintained internal pressure. The surface is discretized into 1200 boundary elements. Discretization, physical properties and other necessary data are displayed in Fig. 3.

In Fig. 4 the radial displacement for the loaded surface is given for three different adopted time steps. As one can observe the displacement results are in good accordance with the analytical solution [16]. It is possible to see that the time marching process is not much sensitive to the time step length, reflecting the stability of the proposed formulation.

Fig. 5 shows the time behaviour of radial and circumferential stress components for a point distant one meter from the loaded surface.

In Fig. 6 the radial displacement values for various points placed along a radial axe of the problem are shown. These values are calculated for the instant  $t = 30$  s and are compared with analytical values.

Physical properties	Geometry
$E_e = 103000.0 \text{ kPa}$	$R = 2.0 \text{ m}$
$\nu = 0.3$	
$\gamma = 6.5 \text{ s}$	
Other parameters	Load
$\Delta t = 0.5 \text{ s}$	$P = 2000.0 \text{ kPa}$
Number of $\Delta t = 160$	

Fig. 3. Buried cavity, physical parameters.

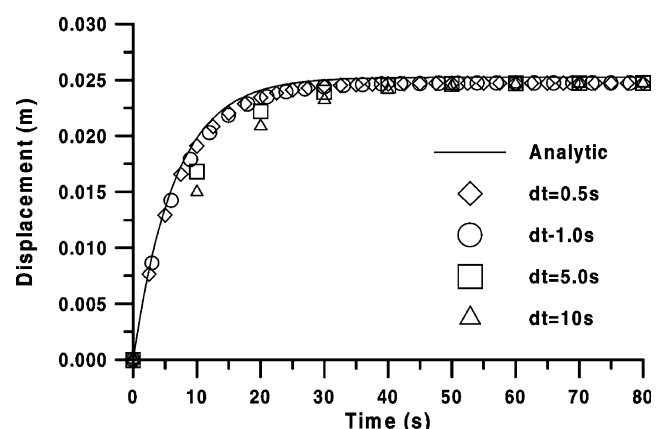


Fig. 4. Radial displacement for the loaded surface.

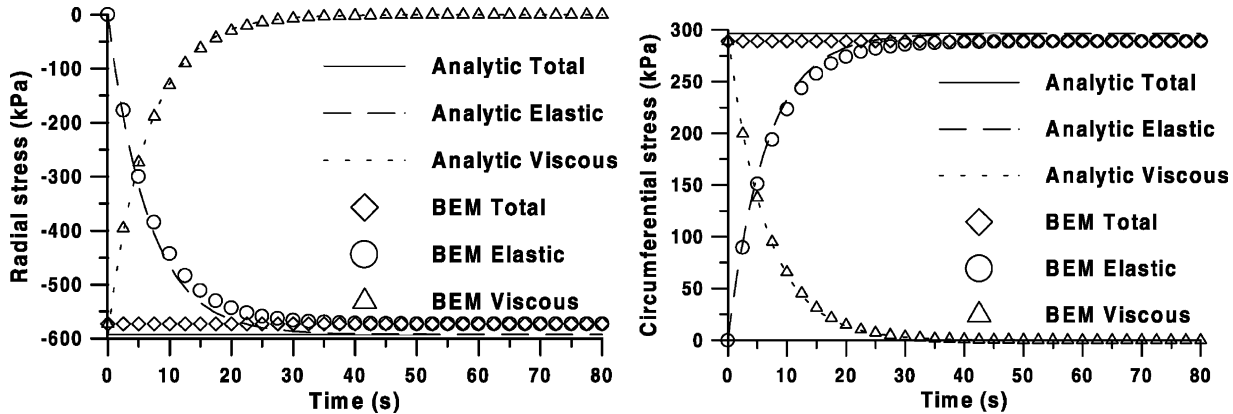
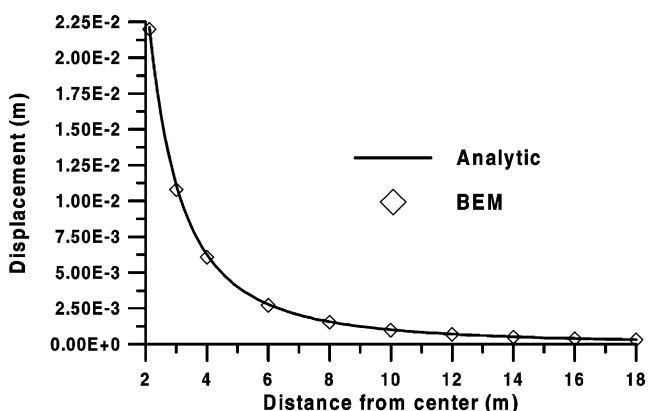


Fig. 5. Time behaviour for radial and circumferential stress components.

From Figs. 5 and 6 one can see the accuracy of the proposed technique.

#### 4.2. Stretched bar 3D (Kelvin)

A bar subjected to a distributed traction at its free extremity is analysed. The structure cross section is square; its surface is modelled by 24 triangular linear boundary elements, see Fig. 7. The adopted model to run this example is the Kelvin viscoelastic one. The geometry and physical parameters are given in Fig. 7.

Fig. 6. Radial displacement for various points along a radial axe ( $t = 30$  s).

The displacement, along time, of the loaded surface is depicted in Fig. 8. As one can observe the proposed technique is able to reproduce perfectly the analytical solution.

The Cartesian longitudinal stress parts, i.e. elastic  $\sigma_{11}^e$ , viscous  $\sigma_{11}^v$  and total  $\sigma_{11}$  at the central point of the structure are shown in Fig. 9.

As demonstrated by these two examples the presented BEM Kelvin viscoelastic formulation is very adequate to solve practical problems.

#### 4.3. Stretched bar (Boltzmann)

The same structure analysed above is now studied adopting the Boltzmann viscoelastic model. The same discretization, loading, Poisson ratio and geometry are adopted. Instantaneous elastic Young modulus  $E_e = 100\,000.0$  Pa and viscoelastic Young modulus  $E_{ve} = 50\,000.0$  Pa are adopted in order to consider the Boltzmann model. Fig. 10 shows the displacement time behaviour of the loaded surface central point. Comparing numerical results with analytical ones it is possible to conclude that the proposed formulation is able to reproduce perfectly both instantaneous and viscous behaviour of the analysed problem. The accuracy is so

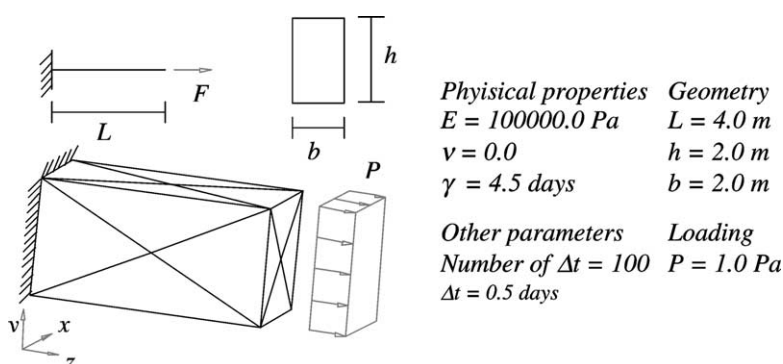


Fig. 7. Geometry, discretization and physical properties of the analysed structure.

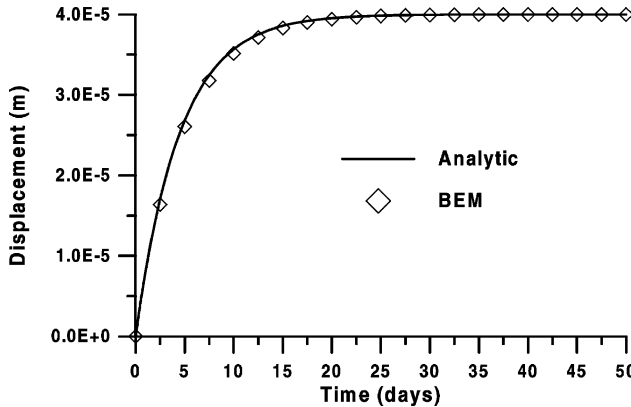


Fig. 8. Displacement of the central point at the loaded surface.

good that is difficult to separate analytical and numerical answers.

The Cartesian longitudinal stress parts, i.e. elastic  $\sigma_{11}^e$ , viscous  $\sigma_{11}^v$  and total  $\sigma_{11}$  at the central point of the structure are shown in Fig. 11.

It is important to note that the instantaneous behaviour of the structure is captured by the time marching procedure

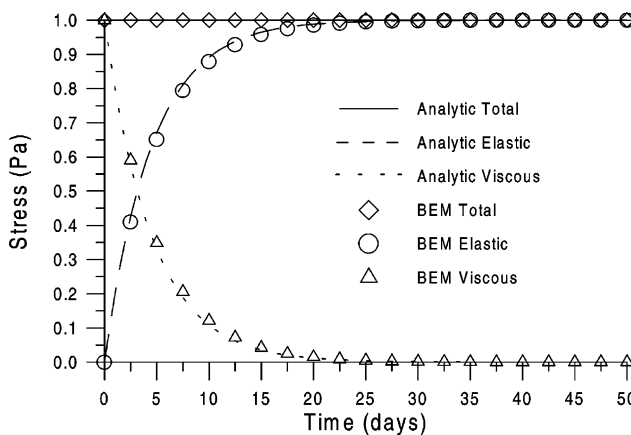
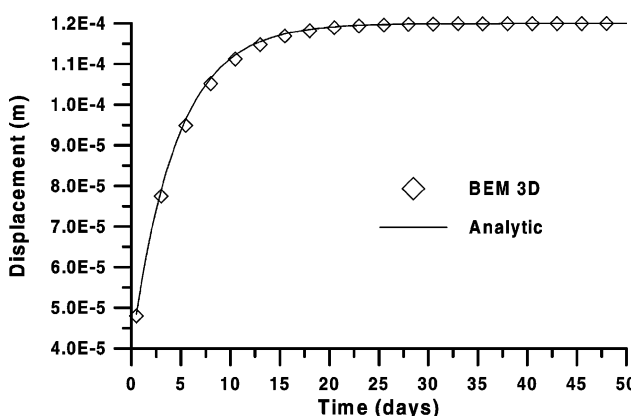
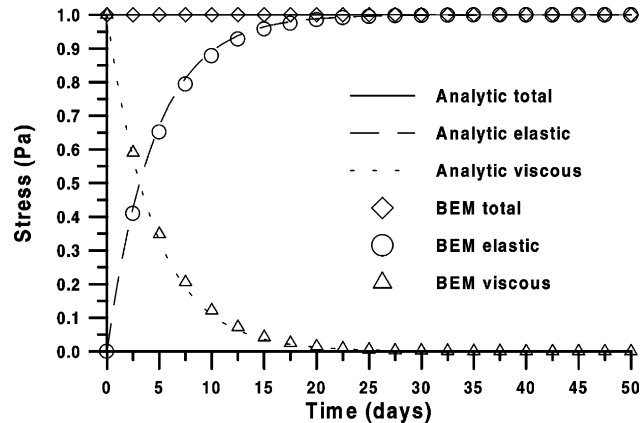
Fig. 9. Elastic stress  $\sigma_{11}^e$ , viscous  $\sigma_{11}^v$  and total  $\sigma_{11}$ , at the centre of the analysed body.

Fig. 10. Displacement of the central point at the loaded surface.

Fig. 11. Elastic stress  $\sigma_{11}^e$ , viscous  $\sigma_{11}^v$  and total  $\sigma_{11}$ , at the centre of the analysed body.

without using any superposition or other extraneous scheme.

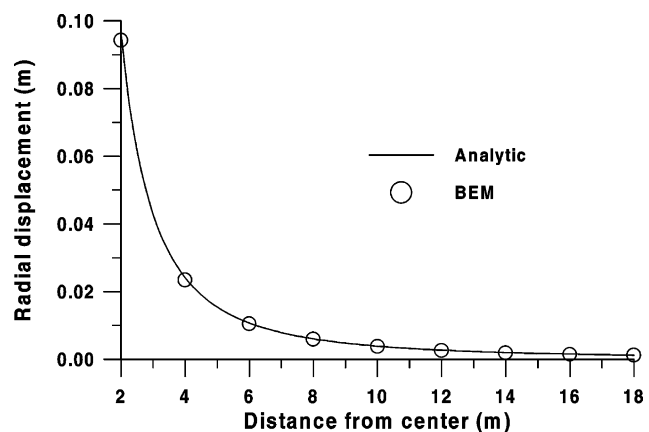
#### 4.4. Spherical cavity (Boltzmann model)

This is the same cavity of Section 4.1, but the material presents instantaneous and viscous Young modulus, i.e. Boltzmann model. Fig. 12 shows all data used to run the analysis.

Fig. 13 presents displacement results for points placed along a radial straight line at  $t = 30$  s. The comparison

Physical properties Geometry	
$E_e = 103000.0 \text{ kPa}$	$R = 2.0 \text{ m}$
$E_{ve} = 35000.0 \text{ kPa}$	
$v = 0.3$	
$\gamma = 6.5 \text{ s}$	
Other parameters	
$\Delta t = 0.5 \text{ s}$	$P = 2000.0 \text{ kPa}$
Number of $\Delta t = 160$	

Fig. 12. Buried cavity physical parameters.

Fig. 13. Displacement versus distance from centre,  $t = 30$  s.

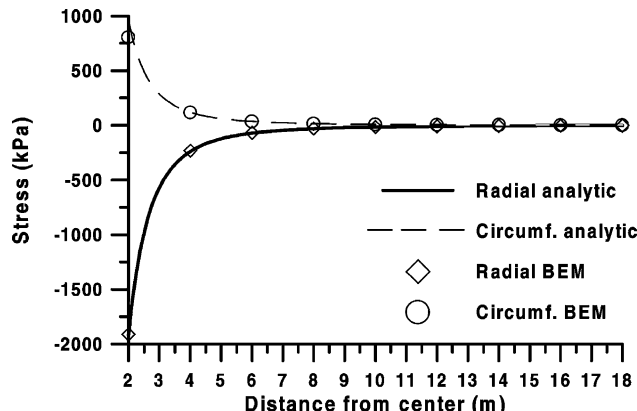


Fig. 14. Radial  $\sigma_r$  and circumferential  $\sigma_\theta$  stresses at  $t = 30$  s.

between numerical values and analytical one demonstrates the accuracy of the proposed technique.

Again as an accuracy measurement, radial and circumferential total stresses along a radial axe are depicted in Fig. 14. These values are in perfect agreement with the analytical solution. The time behaviour for both displacement and stresses are similar to the ones shown for the previous example, and are not presented here in order to save space.

All results demonstrate the very good behaviour of the proposed formulation.

## 5. Conclusions

It has been shown, along the paper, a new way to perform simplified viscoelastic analysis by the boundary element method. It consists in relating the strain time rate with material velocity. From this assumption, the time integration should be done after spatial approximation. Following a weighting residual procedure and a proper kinematical relation between strain and material velocities of neighbour points it is possible to write the boundary integral representation for displacement and stress. The main advantage of the presented technique is that the integral representation posses only boundary values. It has been imposed a spatial approximation for boundary values achieving a system of time differential equations. This system is solved by adopting linear time approximation for both velocity and boundary traction rates.

A very elegant treatment is given for the stress determination. No domain approximations were assumed and only integral equations were applied. Linear time approximation was adopted for stress rates. The proposed formulation has been developed and implemented for both standard Kelvin and Boltzmann viscoelastic models. New research is needed to use this new numerical way of treating viscoelasticity for generalised Kelvin or Maxwell or even any other viscoelastic configuration. The algebraic effort

will not be straightforward, but it is encouraged by the good results obtained here. Four examples are shown and demonstrate the accuracy, stability and generality of the technique.

## Appendix A

### A.1. Some auxiliary values

The not usual functions inside the kernels developed in this work are given by

$$\sigma_{pq}^* = \frac{1}{4\alpha\pi(1-\nu)r^\alpha} [(1-2\nu)(\delta_{pq}r_{,i} + \delta_{iq}r_{,\rho} - \delta_{pi}r_{,q}) + \beta r_{,\rho}r_{,i}r_{,q}] \quad (A1)$$

$$\begin{aligned} p_{pq}^* = & \frac{G}{2\alpha\pi(1-\nu)r^\beta} \left[ \beta \frac{\partial r}{\partial n} \{(1-2\nu)\delta_{pq}r_{,i} \right. \\ & + \nu(\delta_{pi}r_{,q} + \delta_{qi}r_{,\rho}) - \varpi r_{,\rho}r_{,q}r_{,i} \} \\ & + \beta\nu(n_{\rho}r_{,q}r_{,i} + n_{q}r_{,\rho}r_{,i}) \\ & \left. + (1-2\nu)(\beta n_{i}r_{,\rho}r_{,q} + n_{q}\delta_{pi} + n_{\rho}\delta_{qi}) \right. \\ & \left. - (1-4\nu)n_i\delta_{pq} \right] \end{aligned} \quad (A2)$$

$$\bar{B}_{piq}^* = \bar{\sigma}_{piq}^* \frac{\partial r}{\partial n} \quad (A3)$$

where  $(\alpha, \beta, \varpi) = (2, 3, 5)$ .

## References

- [1] Mesquita AD, Coda HB, Venturini WS. An alternative time marching process for viscoelastic analysis by BEM and FEM. *Int J Numer Meth Engng* 2001;51:1157–73.
- [2] Mesquita AD, Coda HB. An alternative time integration procedure for Boltzmann viscoelasticity: a BEM approach. *Comput Struct* 2001;79/16:1487–96.
- [3] Mesquita AD. New methodologies and formulations for inelastic progressive coupling by BEM/FEM. DSc Theses. Universidade de São Paulo, Brazil; 2002 [in Portuguese].
- [4] Mesquita AD. Boundary integral equation method for general viscoelastic analysis. *Int J Solids Struct* 2002;39:2643–64.
- [5] Mesquita AD, Coda HB. Alternative Kelvin viscoelastic procedure for finite elements. *Appl Math Model* 2002;26/4:501–16.
- [6] Lemaitre J, Chaboche JL. Mechanics of solids. Cambridge: Cambridge University Press; 1990.
- [7] Sobotka Z. Rheology of materials and engineering structures. Prague: Elsevier; 1984.
- [8] Sensale B, Partridge PW, Creus GJ. General boundary elements solution for ageing viscoelastic structures. *Int J Numer Meth Engng* 2001;50(6):1455–68.
- [9] Chen WH, Chang CM, Yeh JT. An incremental relaxation finite element analysis of viscoelastic problems with contact and friction. *Comp Meth Appl Mech Engng* 1993;109:315–9.
- [10] Liu Y, Maniati AM, Antes H. Investigation of a Zienkiewicz–Pande yield surface and an elastic–viscoplastic boundary element formulation. *Engng Anal Bound Elem* 2000;24(2):207–11.
- [11] Liu Y. A unified viscoplastic boundary-element approach for residual stress analysis of axisymmetrical bodies under axisymmetrical and

- non-axisymmetrical loads. *Engng Anal Bound Elem* 1994;14(1):25–37.
- [12] Munaiar Neto J. A study of viscoelastic and viscoplastic constitutive models and the use of finite elements algorithms. Doctor in Science Theses. EESC-USP, Brazil; 1998.
- [13] Brebbia CA, Dominguez J. *Boundary elements: an introductory course*, 2nd ed. Great Britain: McGraw-Hill; 1992.
- [14] Brebbia CA, Telles JCF, Wrobel LC. *Boundary element techniques: theory and applications in engineering*. Berlin: Springer; 1984.
- [15] Antes H, Steinfeld B. In: Brebbia CA, Domingues J, Paris F, editors. A boundary formulation study of massive structures static and dynamic behaviour in Proceedings of the Boundary Elements XIV Seville; CMP, Elsevier 1992. p. 27–42.
- [16] Timoshenko SP, Goodier JN. *Theory of elasticity*. Tokyo: McGraw-Hill Kogakusha; 1970.
- [17] Carini A, Diligenzi M, Maier G. Boundary integral equation analysis in linear viscoelasticity: variational and saddle point formulations. *Comput Mech* 1991;8:87–98.
- [18] Carini A, Gioda G. A boundary integral equation technique for viscoelastic stress analysis. *Int J Numer Anal Meth Geomech* 1986;10:585–608.
- [19] Jin F, Pekau OA, Zhang CH. A 2D time-domain boundary element method with damping. *Int J Numer Meth Engng* 2001;51(6):647–61.
- [20] Lee SS. Boundary element analysis of linear viscoelastic problems using realistic relaxation functions. *Comput Struct* 1995;55(6):1027–36.
- [21] Lee SS. Boundary element analysis of the stress singularity at interface corner of viscoelastic adhesive layers. *Int J Solids Struct* 1998;35(13):1385–94.
- [22] Lee SS, Sohn YS, Park SH. On fundamental solutions in time-domain boundary element analysis of linear viscoelasticity. *Engng Anal Bound Elem* 1994;13:211–7.
- [23] Makris N, Zhang J. Time-domain viscoelastic analysis of earth structures. *Earthquake Engng Struct Dyn* 2000;29:745–68.
- [24] Pan E, Sassolas C, Amadei B, Pfeffer WT. A 3D boundary element formulation of viscoelastic media with gravity. *Comput Mech* 1997;19:308–16.
- [25] Rivkin L, Givoli D. An efficient finite element scheme for viscoelasticity with moving boundaries. *Comput Mech* 2000;24:503–12.
- [26] Sim WJ, Kwak BM. Linear viscoelastic analysis in time domain by boundary element method. *Comput Struct* 1998;29:531–9.
- [27] Gaul L, Schanz M. A viscoelastic boundary element formulation in time domain. *Arch Mech* 1994;46(4):583–94.
- [28] Gaul L, Schanz M. A comparative study of three boundary element approaches to calculate the transient response of viscoelastic solids with unbounded domains. *Comput Meth Appl Mech Engng* 1999;179(1/2):111–23.
- [29] Gaul L, Schanz M, Fiedler C. Viscoelastic formulation of BEM in time and frequency domain. *Engng Anal Bound Elem* 1992;10:137–41.
- [30] Kobayashi S, Kawakami T. Application of BE–FE combined method to analysis of dynamic interactions between structures and viscoelastic soil. In: Brebbia CA, Maier G, editors. *Boundary elements VII*, vol. I. Berlin: Springer; 1985. p. 6–12.
- [31] Schanz M. A boundary element formulation in time domain for viscoelastic solids. *Commun Numer Meth Engng* 1999;15:799–809.
- [32] Schanz M. Wave propagation in viscoelastic and poroelastic continua: a boundary element approach. *Lecture notes in applied mechanics*, Berlin: Springer; 2001.
- [33] Schanz M, Antes H. A new visco and elastodynamic time domain boundary element formulation. *Comput Mech* 1997;20(5):452–9.
- [34] Lee SS, Westmann RA. Application of high order quadrature rules to time domain boundary element analysis of viscoelasticity. *IJNME* 1995;38(4):607–29.
- [35] Tanaka M. *Topics in boundary elements*, vol. 3: computational aspects. Berlin: Springer; 1990.